


RESEARCH ARTICLE

LINC00667 regulates MPP⁺-induced neuronal injury in Parkinson's diseaseXinlong Huo¹, Lisong Wang¹, Jiahui Shao¹, Chenhang Zhou¹, Xiaowei Ying¹, Jinhua Zhao² & Xinchun Jin¹ ¹Department of Neurology, The First People's Hospital of Wenling, Wenling, Zhejiang, 317500, China²Department of Neurosurgery, The First People's Hospital of Xianyang, Xianyang, Shaanxi, 712000, China**Correspondence**

Xinchun Jin, Department of Neurology, The First People's Hospital of Wenling, No. 333, Chuanan Road, Wenling, Zhejiang 317500, China. Tel: 0576-89668501; Fax: 89668222; E-mail: xinchengyenr4@163.com

Jinhua Zhao, Department of Neurosurgery, The First People's Hospital of Xianyang, No. 10, Biyuan Road, Qindu District, Xianyang, Shaanxi 712000, China. Tel: 029-33280000; Fax: 029-33280000; E-mail: zhaobi23784142990@163.com

Funding Information

This research did not receive any specific grant from funding agencies in the public, commercial, or not-for-profit sectors.

Received: 15 April 2021; Revised: 29 October 2021; Accepted: 4 November 2021

Annals of Clinical and Translational Neurology 2022; 9(5): 707–721

doi: 10.1002/acn3.51480

Introduction

Parkinson's disease (PD) is an age-related, neurodegenerative illness, and damages motor ability in the central nerve system.¹ The risky factors which may trigger PD mainly include polychlorinated biphenyls, hereditary, metals, and pesticides.² In terms of clinical primary features, PD is characteristic with rest tremor, bradykinesia, and rigidity.³ Pathologically, PD is accompanied with the depletion nerve cells and nerve cells of nigra produce dopamine.⁴ Despite intensive reports in recent literature, the pathogenesis beneath PD remains obscure. The application of 1-methyl-4-phenyl-1,2,3,6-tetrahydropyridine and its corresponding active metabolite, 1-methyl-4-phenylpyridinium (MPP⁺), have been validated to develop the pathophysiological symptoms in PD and they

Abstract

Objective: Parkinson's disease (PD), also known as paralysis tremor, is a chronic disease of the central nervous system. It has been reported that hepatocyte nuclear factor 4 alpha (HNF4A) is upregulated in PD, but its specific function has not been well explored. **Methods:** We established an in vitro PD model in SH-SY5Y cells stimulated with 1-methyl-4-phenylpyridinium (MPP⁺). Meanwhile, the effect of HNF4A on MPP⁺-treated SH-SY5Y cell behavior was monitored by functional assays. Mechanism assays were conducted to verify the relationship among LINC00667/miR-34c-5p/HNF4A. Rescue experiments validated the regulatory mechanism in PD model. **Results:** The results revealed that depletion of HNF4A suppressed cell cytotoxicity and apoptosis caused by MPP⁺. Knockdown of HNF4A recovered MPP⁺-stimulated oxidative stress and neuroinflammation. Mechanically, HNF4A was targeted and inhibited by miR-34c-5p. Furthermore, we found that LINC00667 positively modulated HNF4A expression via sequestering miR-34c-5p in MPP⁺-stimulated SH-SY5Y cells. Interestingly, the data indicated that HNF4A could transcriptionally activate LINC00667 expression. Rescue experiments presented that miR-34c-5p interference or HNF4A overexpression could mitigate the effects of LINC00667 knockdown on cell viability, cytotoxicity, cell apoptosis, oxidative stress, and neuroinflammation in MPP⁺-treated SH-SY5Y cells. **Conclusion:** Our study first proved LINC00667, miR-34c-5p, and HNF4A constructed a positive feedback loop in MPP⁺-treated SH-SY5Y cells, enriching our understanding of PD.

have been broadly applied to create PD model.⁵ Consequently, it is of pivotal significance to prevent MPP⁺-induced neuronal injury for the development of treating this neurodegenerative disorder in the future.

Long noncoding RNAs (lncRNAs) are generally considered as non-translated transcripts and are more than 200 nucleotides in length. Via exploring multiple physiological and pathological processes, it is noted that lncRNAs are identified as crucial modulators from the aspect of epigenetic to posttranscriptional regulations in gene expression.⁶ It is addressed that lncRNAs could positively regulate gene expression via occupying the (microRNA) miRNA-binding sites to obstruct the targeting of miRNA on target mRNA,⁷ which is termed as competing endogenous RNA (ceRNA) mechanism. lncRNAs in relation to tumor development have been extensively unveiled, such

as UCA1⁸ and HOTAIR.⁹ The tight relation of dysregulated lncRNAs with the development of neurodegenerative disease, including PD has been explored and corroborated.^{10,11} As an example, it has been acknowledged that lncRNA NEAT1 can be promoted in MPP⁺-treated PD mice and its suppression could rescue cell viability, hinder cell apoptosis, and decline caspase-3 activity as well as Bax/Bcl-2 ratio in SH-SY5Y cells following MPP⁺ administration.¹² Ni et al have unveiled lncRNA AL049437 promotion and lncRNA AK021630 suppression in the substantia nigra of PD subjects. AL049437 downregulation results in mitochondrial mass and cell viability promotion in SH-SY5Y cells, whereas downregulation of AK021630 leads to the opposite way.¹³ In addition, long intergenic nonprotein coding RNA 667 (LINC00667) is abnormally expressed in chronic renal failure. Its suppression facilitates renal tubular epithelial cell growth and attenuates renal fibrosis.¹⁴ Furthermore, linc00667 has been reported to strengthen the occurrence of vasculogenic mimicry in glioma.¹⁵ LINC00667 is tightly associated with worse prognosis in small hepatocellular carcinoma.¹⁶ In spite of all above-mentioned findings, the literature focusing on LINC00667 function in PD is limited.

Hepatocyte nuclear factor 4 alpha (HNF4A) is substantiated as a nuclear transcription factor, controlling several hepatic gene transcription. For example, HNF4A has been certified to initiate the transcription of miR-101b in Alzheimer's disease.¹⁷ HNF4A modulates the expression of lncRNA NR_023387 via transcriptional initiation in renal cell carcinoma.¹⁸ HNF4a binds to circ_104075 promoter region to facilitate circ_104075 expression in hepatocellular carcinoma.¹⁹ It is also reported that HNF4A participates in acute myeloid leukemia development.²⁰ Regarding its involvement in PD, HNF4A is identified as an essential regulatory hub gene and is overexpressed in PD.^{21,22}

In this work, we tried to monitor the expression and impact of HNF4A on MPP⁺-induced SH-SY5Y cells. Meanwhile, we investigated the potential ceRNA network in PD cells. It was expected that our findings could enrich the current cognition of PD pathogenesis.

Materials and Methods

Cell culture and treatment

SH-SY5Y, the human neuroblastoma cell line, purchased from American Type Culture Collection (ATCC; Manassas, VA), was hatched in the culture medium adding 10 μ mol/L of fresh retinoic acid (Sigma-Aldrich, St. Louis, MO) and 1% fetal bovine serum (FBS; Solarbio, Beijing, China). Cell sample was cultivated in Dulbecco's modified Eagle's medium at 7th day, with 1% antibiotics and 10% FBS in 5% CO₂ at 37°C. To construct in vitro PD cell

model, samples were treated with the MPP⁺ at the concentrations of 0, 0.5, 1, 2, and 4 mmol/L for 48 h, or with the 2 mmol/L of MPP⁺ for 0, 12, 24, 48, and 72 h.

RNA extraction and quantitative real-time polymerase chain reaction (qRT-PCR)

The total RNAs extracted from SH-SY5Y cell samples were achieved by Trizol reagent (Invitrogen, Carlsbad, CA) for generating cDNA by reverse transcription. qPCR assay was performed with SYBR Premix Ex Taq II (Takara, Shiga, Japan), with GAPDH or U6 as the loading control. Relative gene expression was calculated by 2^{- $\Delta\Delta$ Ct} method. Primer sequences of genes involved in this research are listed in Table 1 and Table S1.

Cell transfection

The shRNAs specific to HNF4A, LINC00667, and nonspecific shRNAs as negative control (NC), as well as the pcDNA3.1 vectors targeting HNF4A, LINC00667, and empty vectors as NC, all were produced by Genepharma (Shanghai, China). The interference sequences used for gene downregulation are displayed in Table 2. The miR-34c-5p mimics, miR-449a mimics, and NC mimics, as well as the miR-34c-5p inhibitor and NC inhibitor were also synthesized by Genepharma. Lipofectamine 2000 (Invitrogen) was applied for 48 h transfection as instructed by the supplier.

Cell counting kit-8

Transfected cell samples treated with 2 mmol/L of MPP⁺ for 48 h were seeded into the 96-well plates (5 \times 10³ cells/well) adding 10 μ L of cell counting kit-8

Table 1. Primer sequences used in qRT-PCR assays were demonstrated.

Gene name	Primer sequence
HNF4A	F:TGCGACTCTCCAAAACCCCT R:ATTGCCATCGTCAACACCT
miR-34c-5p	F:GCCGAGgagcagtgtagttg R:CTCAACTGGTGTCTGTGGA
LINC00667	F:GTGGGTAGGAAACAGTCGGG R:CTCAAAGGTGGCCAAAAGCC
LINC00667 promoter P1	F:GACTCGGTAGATGGCTTTCTCT R:TGAGGCTCGATCTGAAGAACA
LINC00667 promoter P2	F:ACATGTTCTTTTCCCTCAGCA R:GCAGAGGTTAAGTAAGACTGCG
U6	F:TCCCTTCGGGACATCCG R:AATTTTGGACATTCTCGATTGT
GAPDH	F:GACAGTCAGCCGCATCTTCT R:GCGCCCAATACGACCAAAATC

Table 2. Sequences for relevant gene knockdown were listed.

Name	Sequence
sh-NC (for HNF4A)	CCGGATCAGTGTATCACAGTATGTCCTCGAGGACATACTGTGATACTGATTTTTTG
sh-HNF4A#1	CCGGAGTCAAAGTCTTGTATCCAGCTCGAGCTGGATAACAAGACTTTGACTTTTTG
sh-HNF4A#2	CCGGGTCTAATGCTCCAGAATGCACCTCGAGGTGCATTCTGGAAGCATTAGATTTTTG
sh-NC (for LINC00667)	CCGGTTCGGAACATGTAAGTAAAGAGCTCGAGCTCTTACTTACATGTCCGACTTTTTG
sh-LINC00667#1	CCGGTTCGGAAGAAAGTCATGTAAGAGCTCGAGCTCTTACATGACTTTCTCGATTTTTG
sh-LINC00667#2	CCGGGTGAAATGTATAAACGAAGTACTCGAGTACTTCGTTTTATACATTTTCATTTTTG

(CCK-8) reagent. Cell viability was monitored by detecting the absorbance at 450 nm wavelength using the microplate reader.

LDH assay

LDH cytotoxicity detection kit from Takara was acquired to assess the release of lactate dehydrogenase (LDH). After transfection, cell samples (3000 per well) in the 96-well plates were incubated all night at 37°C, then exposed to 2 mmol/L of MPP⁺ for 48 h. The supernatant was cultivated with catalyst and dye solution for 30 min in the dark at room temperature, finally analyzed by plate reader.

TUNEL assay

In Situ Cell Death Detection Kit (Roche Diagnostics, Basel in Switzerland, Germany) was prepared for performing terminal deoxynucleotidyl transferase dUTP nick-end labeling (TUNEL) assay in cell samples. Samples (2×10^6 /mL) were first fixed with 4% paraformaldehyde and permeabilized by 0.1% Triton X-100, then exposed to TUNEL reaction mixture for 1 h. Followed by incubation with DAPI, TUNEL-positive cell samples were monitored by the fluorescent microscopy.

Caspase-3 activity detection

Caspase-3 activity detection was implemented by means of Caspase-3 assay kit (Abcam, Cambridge, MA) after cell transfection. The cell samples (3000 per well) in 6-well plates were first treated with 2 mmol/L of MPP⁺ for 48 h, then lysed and centrifuged. Each sample was cultured with DEVD-p-NA substrate and $2 \times$ reaction buffer for 1 h. Eventually, caspase-3 activity was observed under the microplate reader.

ROS generation detection

Reactive oxygen species (ROS) generation detection was conducted under the help of the manual of Reactive Oxygen Species Assay Kit (Solarbio). Cell samples (4×10^5 /mL) treated with DCFH-DA were rinsed in serum-free

culture medium. In the end, fluorescence intensity was recorded by the microplate reader.

SOD activity detection

After being lysed, cell samples (1×10^6 /μL) were centrifuged at 4°C for 10 min, then supernatant was collected to test the superoxide dismutase (SOD) activity in line with the manual of Total Superoxide Dismutase Assay Kit with NBT (Beyotime, Shanghai, China). SOD activity was detected spectrophotometrically.

Western blot

The cellular protein lysates from SH-SY5Y cell samples were acquired by means of RIPA lysis buffer. Later, the extracted proteins were treated with 15% SDS-PAGE gel, and then shifted electrophoretically to PVDF membranes. Next, the obtained membranes were blocked with 5% skim milk. Primary antibodies against loading control GAPDH (ab8245, Abcam, Cambridge, MA) and IL-6 (ab233706, Abcam), IL-1β (ab254360, Abcam), TNF-α (ab183218, Abcam), along with the corresponding secondary antibodies (ab7090, Abcam) were utilized after dilution. Western band was analyzed with enhanced chemiluminescence Western Blotting Detection Kit (Solarbio).

Dual-luciferase reporter assay

The pmirGLO Vector (Promega, Madison, WI) containing HNF4A 3'UTR was co-transfected with miR-34c-5p mimics, miR-449a mimics, or NC mimics in 3×10^3 SH-SY5Y cell samples. Wild-type (WT) and mutated (MUT) miR-34c-5p binding sites in HNF4A or LINC00667 fragments were sub-cloned into the pmirGLO Vector to construct pmirGLO-HNF4A-WT/MUT and pmirGLO-LINC00667-WT/MUT. In addition, the WT or MUT HNF4A-binding sites in LINC00667 promoter were synthesized and cloned to pGL3 Vector (Promega), then co-transfected with pcDNA3.1/HNF4A, sh-HNF4A, or their relative NC. Dual-Luciferase Assay System (Promega) was finally employed for detecting luciferase intensity.

RNA binding protein immunoprecipitation (RIP) assay

5×10^6 cell samples were involved in this assay. EZ-Magna RIP RNA Binding Protein Immunoprecipitation Kit was obtained from Millipore (Bedford, MA) for performing RIP analysis. Briefly speaking, SH-SY5Y cells were lysed first and then incubated with human Argonaute 2 (Ago2) antibody (MABE-253, Sigma-Aldrich) or NC normal mouse immunoglobulin G antibody (IgG; ab172730, Abcam). Eventually, purified precipitates were assayed by qRT-PCR.

Subcellular fractionation

Nuclear and cytoplasmic fractions were both isolated from 3×10^6 cell samples in light of the guidebook of PARIS™ Kit (Invitrogen). LINC00667 level in different parts was detected by qRT-PCR, and standardized to GAPDH (cytoplasmic control) and U6 (nuclear control).

ChIP assay

After crosslinking, 5×10^5 chromatin samples were broken for immunoprecipitation with anti-HNF4A antibody (ab181604, Abcam) or control anti-IgG antibody (ab172730, Abcam). The antibodies used herein were all chromatin immunoprecipitation (ChIP) Grade. The sample was subjected to 14 times of sonication cycles every 9 sec. Followed by incubation with Protein A/G mix magnetic beads for an hour, precipitated samples were collected for qRT-PCR analysis.

Statistical analyses

Results were exhibited as the Mean \pm SD of bio-triple repeats. Data were processed statistically by *t*-test, one-way analysis of variance (ANOVA) or two-way ANOVA by application of Prism software 6.0 (GraphPad, San Diego, CA), with $p < 0.05$ as significant level. Dunnett's *t*-test or Tukey was used to verify the data difference after ANOVA analysis. The post-hoc tests were run only if *F* achieved $p < 0.05$ and there was no significant variance inhomogeneity.

Results

Depletion of HNF4A led to recovery from MPP⁺-mediated neuronal injury

As reported previously, HNF4A, a transcription factor, was identified as an actively expressed gene in PD patients.²² Herein, we aimed to explore the potential

function of HNF4A in PD. First of all, an in vitro cell model of PD was constructed in SH-SY5Y cells treated with indicated concentrations of MPP⁺ or treated with MPP⁺ for different time. At cellular level, we observed that the expression of HNF4A was increased in PD cell model in a dose- or time-dependent manner (Fig. 1A and B). Following that, loss-of function experiments were implemented with the transfection of sh-HNF4A#1/2 plasmids. After 48-h transfection, HNF4A was dramatically reduced in sh-HNF4A#1/2 group, compared with blank or NC group (Fig. 1C). Before functional assays, transfected cells were treated with MPP⁺ (2 mmol/L) for 48 h. As presented in CCK-8 assay, MPP⁺-caused suppression on cell viability was alleviated by HNF4A depletion (Fig. 1D). SH-SY5Y cytotoxicity induced by MPP⁺ was detected by means of LDH cytotoxicity detection kit. As a consequence, it turned out that the increase of LDH release caused by MPP⁺ could be recovered via HNF4A knockdown (Fig. 1E). In terms of SH-SY5Y apoptosis, TUNEL and caspase-3 activity analyses demonstrated that the treatment of MPP⁺ resulted in stimulated apoptosis of SH-SY5Y, while HNF4A knockdown effectively counteracted this effect (Fig. 1F and G). Additionally, we also evaluated oxidative stress in SH-SY5Y following MPP⁺ administration. Oxidative stress manifests as elevation of ROS and reduction in SOD.²³ The following results also displayed a marked enhancement of ROS generation and conversely a reduction of SOD activity upon MPP⁺ administration. However, depletion of HNF4A restored MPP⁺-caused oxidative stress, as supported by repressed ROS generation and facilitated SOD activity (Fig. 1H and I). Furthermore, we also tried to figure out the function of HNF4A in MPP⁺-stimulated neuroinflammation. Therefore, the expression of three pro-inflammatory cytokines (TNF- α , IL-1 β , and IL-6) was examined by means of western blot. MPP⁺ treatment led to an augmentation of pro-inflammatory cytokine expression while HNF4A deficiency effectively suppressed the former impact (Fig. 1J and Fig. S1A). Overall, knockdown of HNF4A counteracted the MPP⁺-induced decrease of cellular viability and increase of apoptosis, cytotoxicity, oxidative stress as well as neuroinflammation in SH-SY5Y cells.

HNF4A was targeted by miR-34c-5p

The outcomes obtained from ENCORI (<http://starbase.sysu.edu.cn/>), microRNA.org (<http://www.microRNA.org/microRNA/home.do>), and miRDB (<http://mirdb.org/>) algorithms unveiled that two miRNAs (miR-34c-5p and miR-449a) were predicted to possibly target HNF4A (Fig. 2A). To determine the specific miRNA that could bind to HNF4A, we performed the luciferase reporter assay. The results indicated that miR-34c-5p mimics

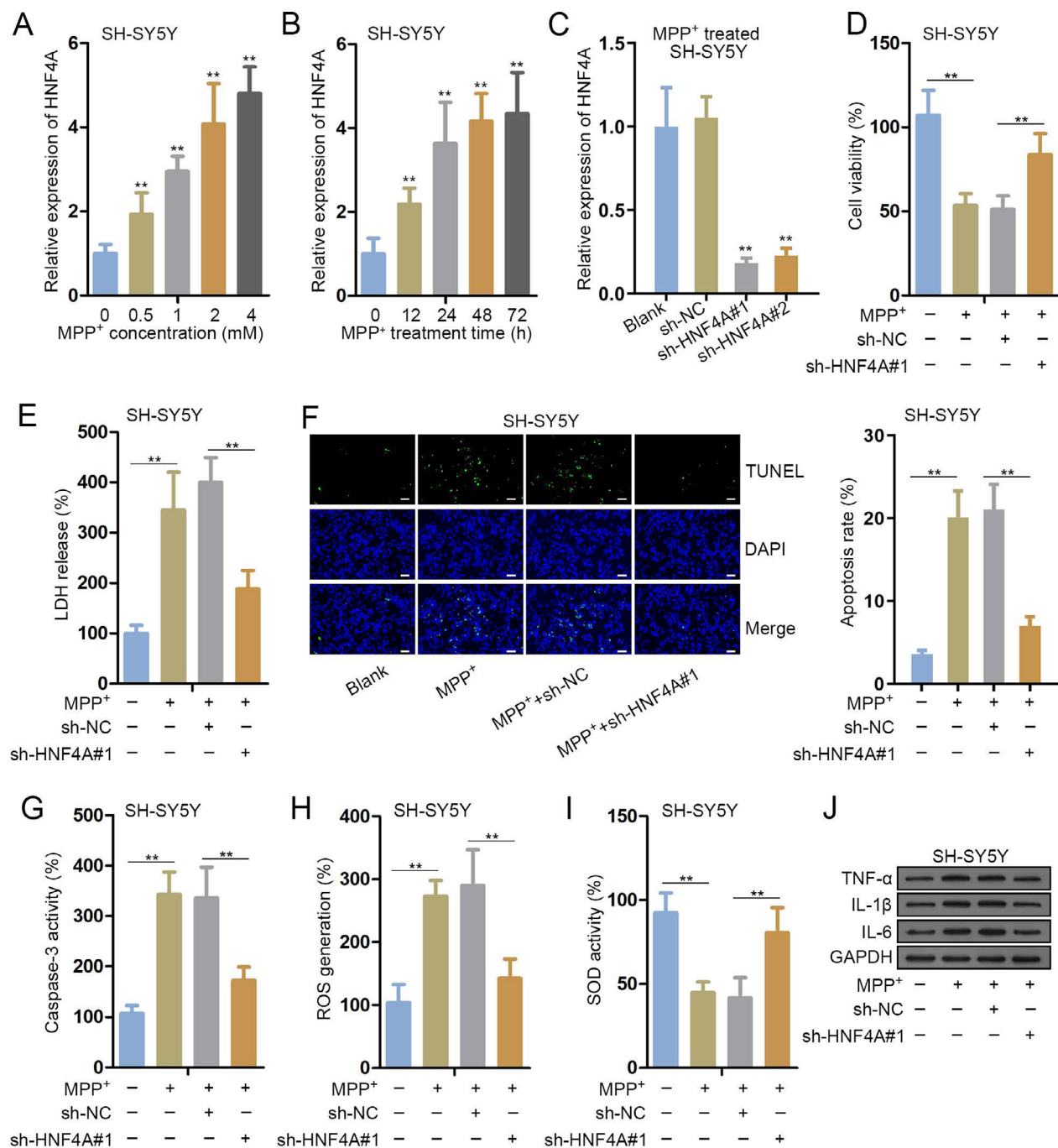
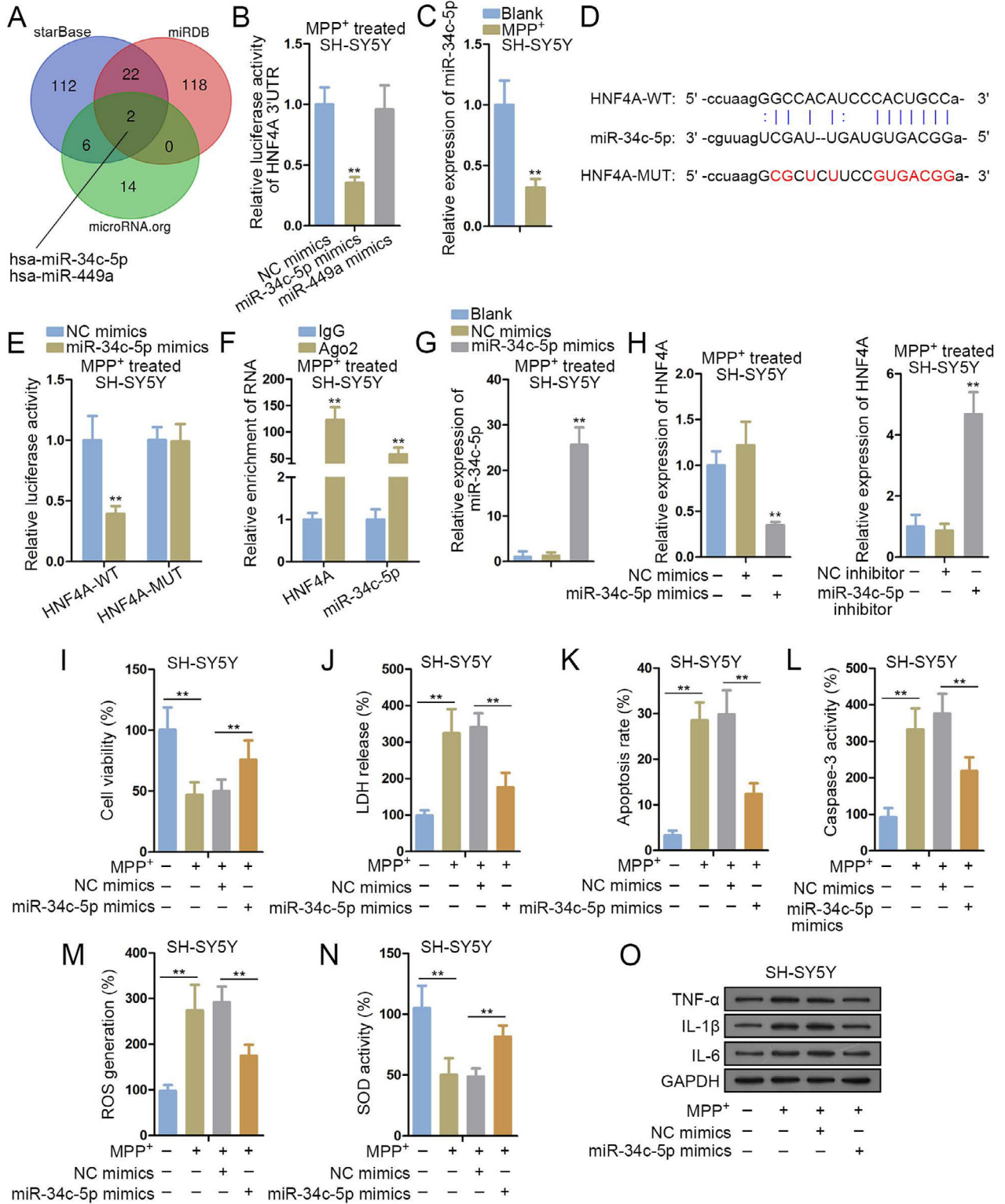


Figure 1. Depletion of HNF4A led to recovery from MPP⁺-mediated neuronal injury. (A) MPP⁺ was utilized for SH-SY5Y cell treatment for 48 h with different concentrations (0, 0.5, 1, 2, and 4 mmol/L); treated SH-SY5Y cells underwent qRT-PCR analysis for HNF4A expression. (B) 2 mmol/L MPP⁺-treated SH-SY5Y cells for indicated times (0, 12, 24, 48, and 72 h); treated SH-SY5Y cells underwent qRT-PCR analysis for HNF4A expression. (C) Transfection efficiency of sh-HNF4A#1/2 for HNF4A knockdown was examined by qRT-PCR. (D) Following MPP⁺ treatment, SH-SY5Y cells transfected with sh-NC or sh-HNF4A#1 were engaged in CCK-8 assay of SH-SY5Y cell viability. (E) LDH cytotoxicity detection kit was utilized to detect LDH release in MPP⁺-treated SH-SY5Y cells transfected with sh-HNF4A#1. (F and G) Apoptosis of SH-SY5Y cells and apoptosis-related protein caspase-3 activity upon indicated treatments were examined through TUNEL and western blot assays. (H and I) ROS generation and SOD activity were assessed utilizing commercial assay kits in SH-SY5Y cells. (J) Western blot was conducted to detect the protein levels of TNF- α , IL-1 β , and IL-6. ** $p < 0.01$. HNF4A, hepatocyte nuclear factor 4 alpha; MPP⁺, 1-methyl-4-phenylpyridinium; qRT-PCR, quantitative real-time polymerase chain reaction; CCK-8, cell counting kit-8; LDH, lactate dehydrogenase; TUNEL, terminal deoxynucleotidyl transferase dUTP nick-end labeling; ROS, reactive oxygen species; SOD, superoxide dismutase.



rather than miR-449a mimics could weaken the luciferase activity of HNF4A 3'UTR (Fig. 2B). In addition, MPP⁺ administration resulted in miR-34c-5p

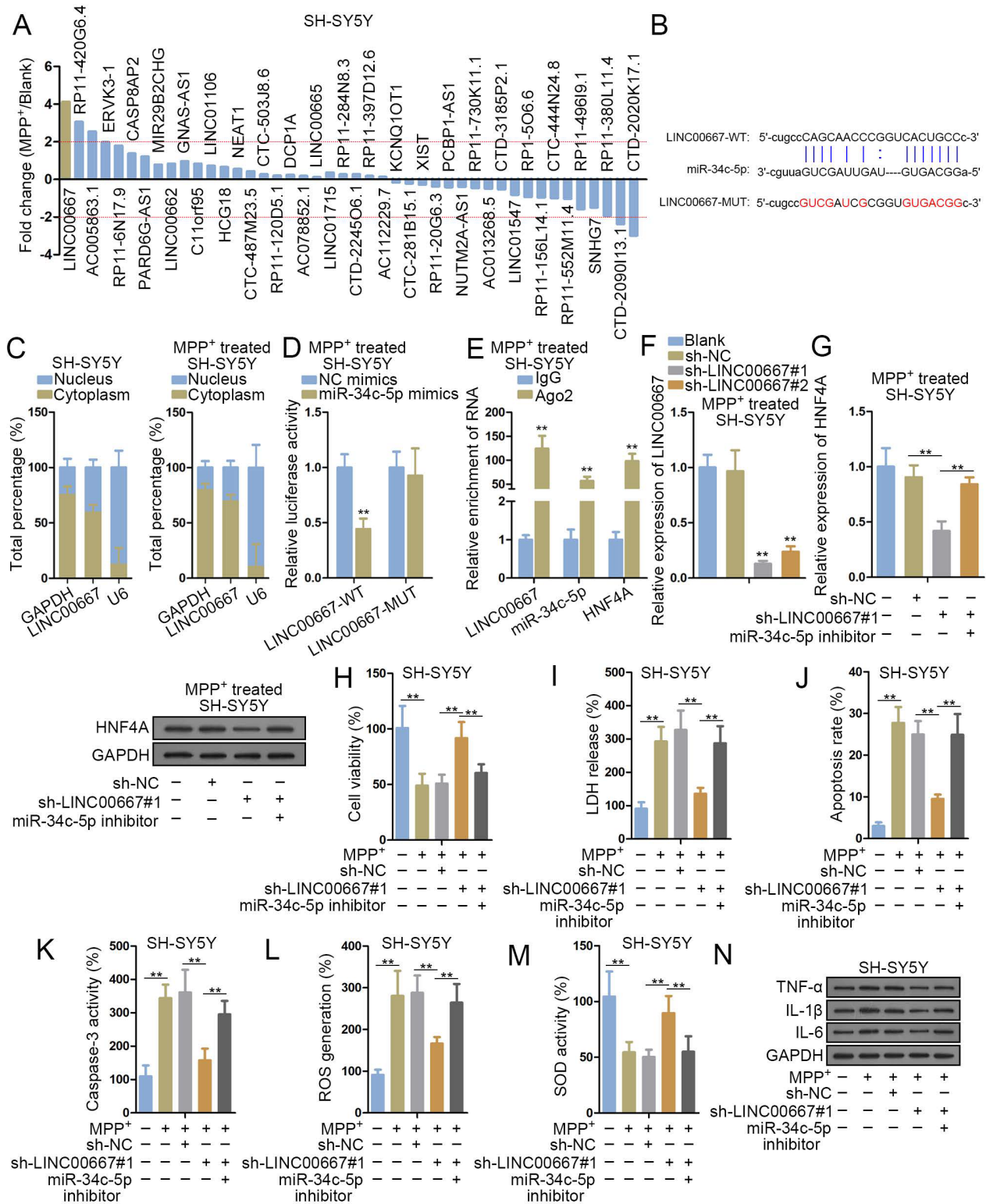
downregulation, compared with untreated group (Fig. 2C). Therefore, miR-34c-5p was confirmed as the target miRNA involved in the subsequent research.

Figure 2. HNF4A was targeted by miR-34c-5p. (A) ENCORI, microRNA.org, and miRDB were utilized to predict the candidate miRNAs targeting HNF4A. (B) Luciferase activity of HNF4A 3'UTR in the presence of miR-34c-5p mimics or miR-449a mimics was examined through dual-luciferase reporter assay in SH-SY5Y cells treated with MPP⁺. (C) In SH-SY5Y cells, miR-34c-5p expression upon MPP⁺ stimulation was evaluated in qRT-PCR. (D) Bioinformatics tool was utilized to predict the binding sites between the 3'UTR region of HNF4A and miR-34c-5p. (E) Dual-luciferase reporter assay was performed to examine the binding affinity between HNF4A-WT/MUT and miR-34c-5p in SH-SY5Y cells. (F) RIP was conducted to test the binding affinity of HNF4A and miR-34c-5p in SH-SY5Y cells. (G) The transfection efficiency of miR-34c-5p mimics was examined by qRT-PCR in SH-SY5Y cells. (H) In SH-SY5Y cells, qRT-PCR was done to detect expression of HNF4A after miR-34c-5p upregulation upon MPP⁺ treatment. (I) CCK-8 assay was carried out to evaluate the impact of miR-34c-5p elevation on cell viability in MPP⁺-induced SH-SY5Y cells. (J) The influence of miR-34c-5p elevation on LDH release in MPP⁺-treated SH-SY5Y cells was assessed. (K and L) The effects of miR-34c-5p augmentation on MPP⁺-intoxicated SH-SY5Y cell apoptosis was evaluated through TUNEL and western blot assays. (M and N) Upon miR-34c-5p upregulation, ROS generation and SOD activity in MPP⁺-intoxicated SH-SY5Y cells was examined respectively. (O) Western blot analysis of TNF-, IL-1, and IL-6 levels following miR-34c-5p overexpression in MPP⁺-intoxicated SH-SY5Y cells was done. ***p* < 0.01. HNF4A, hepatocyte nuclear factor 4 alpha; MPP⁺, 1-methyl-4-phenylpyridinium; qRT-PCR, quantitative real-time polymerase chain reaction; RIP, RNA binding protein immunoprecipitation; CCK-8, cell counting kit-8; LDH, lactate dehydrogenase; TUNEL, terminal deoxynucleotidyl transferase dUTP nick-end labeling; ROS, reactive oxygen species; SOD, superoxide dismutase.

Bioinformatics analysis exhibited the 3'UTR region of HNF4A that contained miR-34c-5p binding affinity (Fig. 2D). Luciferase reporter analysis described that miR-34c-5p upregulation decreased the luciferase activity of reporters cloned with HNF4A-WT. And miR-34c-5p mimics had no impact on the luciferase activity of HNF4A-MUT (Fig. 2E). Previously, miRNAs could employ the RNA-induced silencing complex (RISC), of which the core element is Ago2, to posttranscriptionally suppress target mRNA expression.²⁴ Therefore, we utilized Ago2-RIP to assess their interaction in RISC. The results from RIP assay manifested that HNF4A and miR-34c-5p were abundant in the mixture precipitated by anti-Ago2 (Fig. 2F). To validate the inverse regulation of miR-34c-5p on HNF4A, we firstly examined the successful upregulation by miR-34c-5p mimics (Fig. 2G). Additionally, data from qRT-PCR displayed that transfection of miR-34c-5p mimics repressed HNF4A mRNA while miR-34c-5p inhibitor prominently enhanced HNF4A mRNA level (Fig. 2H). Functionally, we illustrated the functional importance of miR-34c-5p in MPP⁺-induced neuronal injury in SH-SY5Y cells. In CCK-8 assay, elevation of miR-34c-5p boosted cell viability of MPP⁺-induced SH-SY5Y cells (Fig. 2I). Meanwhile, miR-34c-5p overexpression was accompanied with the decline of LDH release in MPP⁺-treated SH-SY5Y cells (Fig. 2J). SH-SY5Y cells under MPP⁺ treatment underwent inhibited apoptosis when miR-34c-5p was upregulated, as demonstrated in TUNEL and caspase-3 activity assays (Fig. 2K and L). MiR-34c-5p elevation hindered ROS generation while facilitating SOD activity in SH-SY5Y cells stimulated by MPP⁺ (Fig. 2M and N). Moreover, miR-34c-5p mimics exerted suppressive effect on TNF- α , IL-1 β , and IL-6 protein expression in SH-SY5Y cells following MPP⁺ treatment (Fig. 2O and Fig. S1B). Collectively, miR-34c-5p bound to HNF4A and repressed MPP⁺-mediated neuronal injury in SH-SY5Y cells.

LINC00667 sponged miR-34c-5p and aggravated MPP⁺-mediated neuronal injury

Based on current knowledge, lncRNAs could also exert their function in RISC through sponging miRNAs.²⁵ Therefore, investigations were conducted to screen out theoretical upstream lncRNA of miR-34c-5p. StarBase (<http://starbase.sysu.edu.cn/starbase2/rbpMrna.php>) predicted 44 lncRNAs which may interact with miR-34c-5p. Subsequently, the expression of 44 lncRNAs following MPP⁺ treatment was verified in qRT-PCR. We noticed that LINC00667 was the most increased lncRNA upon MPP⁺ administration, as a result of which it was selected as the potential upstream gene of miR-34c-5p (Fig. 3A). The interacting sequence between LINC00667 and miR-34c-5p was demonstrated (Fig. 3B). Whether LINC00667 could function as a miRNA-sponging lncRNA depended on its cellular distribution. Consequently, SH-SY5Y cells with or without MPP⁺ treatment underwent subcellular fractionation assay. The outcomes exhibited that LINC00667 was primarily located in the cytoplasmic part (Fig. 3C). In luciferase reporter assay, we sub-cloned LINC00667-WT and LINC00667-MUT into luciferase reporters, followed by the transfection of miR-34c-5p mimics. As a result, the luciferase activity declined in SH-SY5Y cells co-transfected with luciferase reporter containing LINC00667-WT and miR-34c-5p mimics. However, the luciferase activity of LINC00667-MUT reporter was unaffected by miR-34c-5p mimics (Fig. 3D). Meanwhile, data from RIP indicated that LINC00667, miR-34c-5p, and HNF4A co-existed in RISC (Fig. 3E). Next, to certify the modulation of LINC00667 on HNF4A expression through miR-34c-5p, we ectopically reduced LINC00667 expression via sh-LINC00667#1/2 transfection in MPP⁺-treated SH-SY5Y cells (Fig. 3F). Later, it was found that transfection of sh-LINC00667#1 led to HNF4A mRNA and protein downregulation while repression of miR-34c-5p relieved



the effects caused by sh-LINC00667#1 (Fig. 3G and Fig. S1C). Subsequently, we tried to figure out whether LINC00667 functioned through miR-34c-5p in MPP⁺-

treated SH-SY5Y cells. The data of CCK-8 assay showed that in the presence of MPP⁺, LINC00667 depletion increased SH-SY5Y cell viability, while miR-34c-5p

Figure 3. LINC00667 sponged miR-34c-5p and aggravated MPP⁺-mediated neuronal injury. (A) 44 lncRNAs were obtained from bioinformatics predications. The expression of 44 candidate lncRNAs upon MPP⁺ stimulation was analyzed by qRT-PCR. (B) The binding sequence between LINC00667 and miR-34c-5p was predicted by starBase. (C) Subcellular fractionation assay was performed to confirm the distribution of LINC00667 in SH-SY5Y or MPP⁺-treated SH-SY5Y cells. (D) The impacts of miR-34c-5p mimics on luciferase activity of LINC00667-WT or LINC00667-MUT were examined by dual-luciferase reporter assays in MPP⁺-treated SH-SY5Y cells. (E) RIP assay was performed to confirm the co-existence of LINC00667, miR-34c-5p, and HNF4A in the same RISC complex. (F) The knockdown efficiency of sh-LINC00667#1/2 was examined via qRT-PCR. (G) The RNA and protein levels of HNF4A were detected via qRT-PCR and western blot assays in response to sh-NC, sh-LINC00667#1, or sh-LINC00667#1+miR-34c-5p inhibitor in MPP⁺-induced SH-SY5Y cells. (H) CCK-8 was performed to estimate cell viability of MPP⁺-intoxicated SH-SY5Y cells transfected with different plasmids. (I) LDH release in specifically treated SH-SY5Y cells was monitored. (J and K) Apoptosis rate and caspase-3 activity of specifically treated SH-SY5Y cell was examined by TUNEL and western blot assays. (L and M) ROS generation and SOD activity in specifically treated SH-SY5Y cells was detected in SH-SY5Y cells. (N) Western blot assay was operated to detect the protein levels of TNF- α , IL-1 β , and IL-6 in specifically treated SH-SY5Y cells. ** $p < 0.01$. MPP⁺, 1-methyl-4-phenylpyridinium; qRT-PCR, quantitative real-time polymerase chain reaction; RIP, RNA binding protein immunoprecipitation; RISC, RNA-induced silencing complex; HNF4A, hepatocyte nuclear factor 4 alpha; CCK-8, cell counting kit-8; LDH, lactate dehydrogenase; TUNEL, terminal deoxynucleotidyl transferase dUTP nick-end labeling; ROS, reactive oxygen species; SOD, superoxide dismutase; lncRNAs, long noncoding RNAs.

inhibition reversed the effects of sh-LINC00667#1 (Fig. 3H). Moreover, the reduced release of LDH caused by sh-LINC00667#1 could be restored by miR-34c-5p inhibitor (Fig. 3I). Results of TUNEL and caspase-3 activity assays indicated that sh-LINC00667#1 reduced the apoptotic rate of MPP⁺-treated SH-SY5Y cells while downregulation of miR-34c-5p mitigated the apoptotic trend of MPP⁺-treated SH-SY5Y cells (Fig. 3J and K). In addition, increased ROS generation in MPP⁺-treated SH-SY5Y cells was restrained by sh-LINC00667#1 while miR-34c-5p inhibitor countervailed the effects of sh-LINC00667#1 (Fig. 3L). Next, it was revealed the upturned SOD activity in MPP⁺-treated SH-SY5Y cells induced by sh-LINC00667#1 was further recovered by miR-34c-5p inhibitor (Fig. 3M). Moreover, LINC00667 deficiency gave rise to the decrease of pro-inflammatory protein content which was restored by miR-34c-5p suppression (Fig. 3N and Fig. S1D). Taken together, miR-34c-5p offset the facilitating effect of LINC00667 on MPP⁺-stimulated neuronal injury.

LINC00667 positively regulated HNF4A in MPP⁺-caused neuronal injury

To confirm that LINC00667 regulated HNF4A to affect neuronal injury in MPP⁺-treated SH-SY5Y cells, rescue experiments were further conducted. HNF4A was first ectopically augmented via HNF4A-overexpressing vectors (Fig. 4A). Later, it was revealed in CCK-8 that the promoting effect of sh-LINC00667#1 on cell viability was reversed by HNF4A overexpression (Fig. 4B). Meanwhile, the suppressive impact of sh-LINC00667#1 on cytotoxicity was counteracted by HNF4A overexpression (Fig. 4C). Simultaneously, reduced apoptosis of MPP⁺-induced SH-SY5Y cells following LINC00667 depletion was recovered via HNF4A augmentation (Fig. 4D and E). HNF4A augmentation abolished the inhibitory impact of LINC00667 depletion on ROS generation and

promoting effect on SOD activity (Fig. 4F and G). Moreover, it was found that the protein level of TNF- α , IL-1 β , and IL-6 declined upon LINC00667 depletion, while being increased via pcDNA3.1/HNF4A (Fig. 4H and Fig. S1E). Collectively, inhibition of LINC00667 resulted in an obvious restriction on neuronal injury in MPP⁺-intoxicated SH-SY5Y cells while pcDNA3.1/HNF4A antagonized the effects.

HNF4A transcriptionally activated LINC00667 expression

Previously, HNF4A was certified to initiate the transcription of miRNA, lncRNA, and circRNA.^{17–19} We speculated HNF4A might be responsible for LINC00667 upregulation in PD. JASPAR (<http://jaspar.genereg.net/>) exhibited the DNA motif of HNF4A (Fig. 5A). Meanwhile, the potential HNF4A-binding sequence within LINC00667 promoter included P1 (+1 to –1100) and P2 (–1000 to –2000) (Fig. 5B). ChIP assay verified that P2 region (–1000 to –2000) of LINC00667 promoter contained the HNF4A-binding motif as only the P2 part was largely enriched in anti-HNF4A (Fig. 5C). To further confirm whether HNF4A-binding motif was in site 3 or site 4, luciferase reporters containing LINC00667 promoter-WT, LINC00667 promoter-MUT, LINC00667 promoter-site 3-MUT, or site 4-MUT were constructed. We observed that luciferase activity of LINC00667 promoter-WT was stimulated via pcDNA3.1/HNF4A. Similar result was observed in site 3-MUT group. But when the full length or site 4 of LINC00667 promoter was MUT, the luciferase activity could not be stimulated by pcDNA3.1/HNF4A (Fig. 5D). Conversely, luciferase activity of LINC00667 promoter-WT or LINC00667 promoter-site 3-MUT was reduced by sh-HNF4A#1. But the luciferase activity of other two groups was not modulated by sh-HNF4A#1 (Fig. 5E). The results of Figure 5D and E jointly confirmed the binding site of HNF4A on

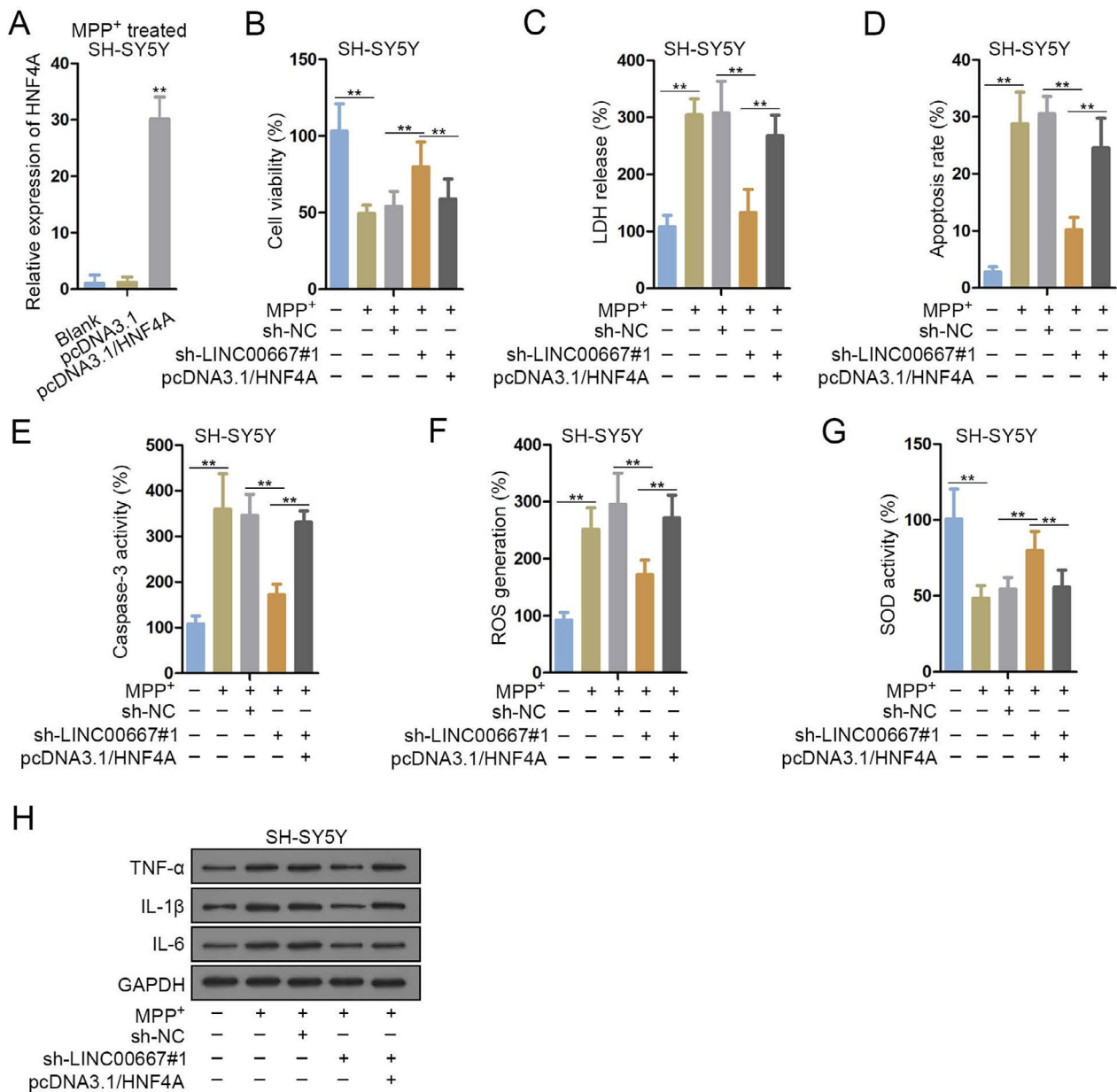


Figure 4. LINC00667 positively regulated HNF4A in MPP⁺-caused neuronal injury. (A) The overexpression efficiency of pcDNA3.1/HNF4A in MPP⁺-treated SH-SY5Y cells was tested by qRT-PCR. (B) MPP⁺-intoxicated SH-SY5Y cells were transfected with sh-NC, sh-LINC00667#1, or sh-LINC00667#1+pcDNA3.1/HNF4A; CCK-8 was carried out to monitor SH-SY5Y cell viability following different treatments. (C) LDH release in specifically treated SH-SY5Y cells was monitored. (D and E) With different treatments, apoptosis rate, and caspase-3 activity analyses were detected through TUNEL and western blot assays in SH-SY5Y cells. (F and G) ROS generation and SOD activity were detected in SH-SY5Y cells with different plasmids. (H) Western blot analysis of TNF-α, IL-1β, and IL-6 levels was done in SH-SY5Y cells lured by MPP⁺. ***p* < 0.01. HNF4A, hepatocyte nuclear factor 4 alpha; MPP⁺, 1-methyl-4-phenylpyridinium; qRT-PCR, quantitative real-time polymerase chain reaction; CCK-8, cell counting kit-8; LDH, lactate dehydrogenase; TUNEL, terminal deoxynucleotidyl transferase dUTP nick-end labeling; ROS, reactive oxygen species; SOD, superoxide dismutase.

LINC00667 promoter was Site 4. Moreover, at molecular level, pcDNA3.1/HNF4A boosted LINC00667 expression to a great extent, whereas sh-HNF4A#1 overtly repressed LINC00667 transcription (Fig. 5F). To sum up, LINC00667 transcription was activated by HNF4A.

HNF4A-mediated LINC00667 elevation exacerbated MPP⁺-caused neuronal injury

To validate HNF4A modulated LINC00667 in MPP⁺-caused neuronal injury, we employed rescue assays. First,

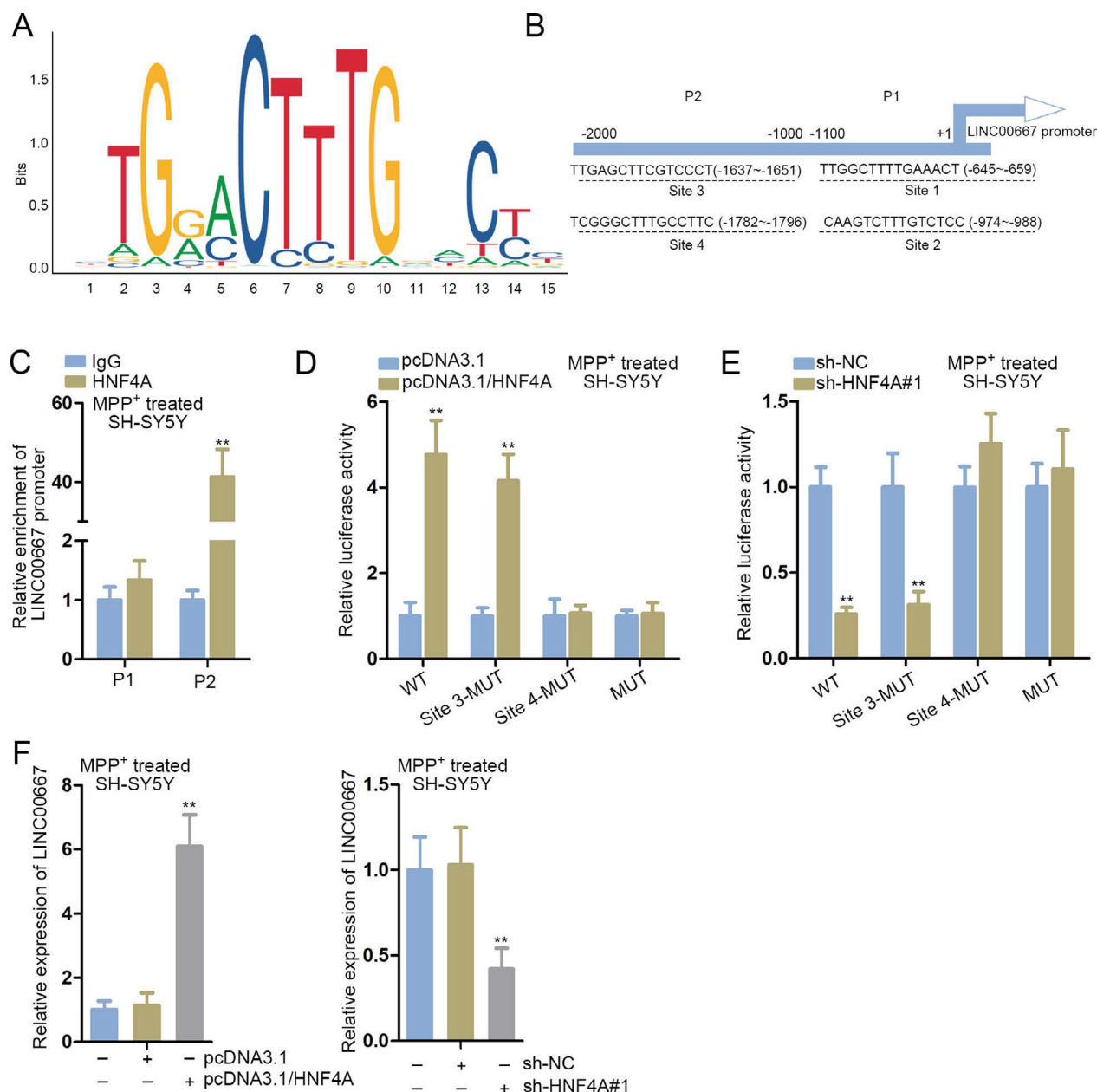


Figure 5. HNF4A transcriptionally initiated LINC00667 expression. (A) HNF4A DNA motif from JASPAR was displayed. (B) HNF4A-binding motif in LINC00667 promoter was presented. (C) ChIP assay was performed to verify the binding affinity of LINC00667 promoter and HNF4A protein in MPP⁺-treated SH-SY5Y cells. (D) Luciferase activity of LINC00667 promoter with or without indicated mutations in the presence of pcDNA3.1/HNF4A was detected via dual-luciferase reporter assay in MPP⁺-treated SH-SY5Y cells. (E) Luciferase activity of LINC00667 promoter with or without indicated mutations in the presence of sh-HNF4A#1 was tested through dual-luciferase reporter assay in MPP⁺-treated SH-SY5Y cells. (F) In MPP⁺-treated SH-SY5Y cells, qRT-PCR was implemented to quantify the expression of LINC00667 upon HNF4A overexpression or depletion. ** $p < 0.01$. HNF4A, hepatocyte nuclear factor 4 alpha; MPP⁺, 1-methyl-4-phenylpyridinium; ChIP, chromatin immunoprecipitation; qRT-PCR, quantitative real-time polymerase chain reaction.

pcDNA3.1/LINC00667 was transfected into SH-SY5Y cells for LINC00667 upregulation (Fig. 6A). Subsequently, results of CCK-8 manifested that depletion of HNF4A led to promoted viability of MPP⁺-intoxicated SH-SY5Y cells

but pcDNA3.1/LINC00667 abrogated the stimulation on cell viability (Fig. 6B). The release of LDH in MPP⁺-intoxicated SH-SY5Y cells was repressed by HNF4A knockdown, while the repression on LDH release was

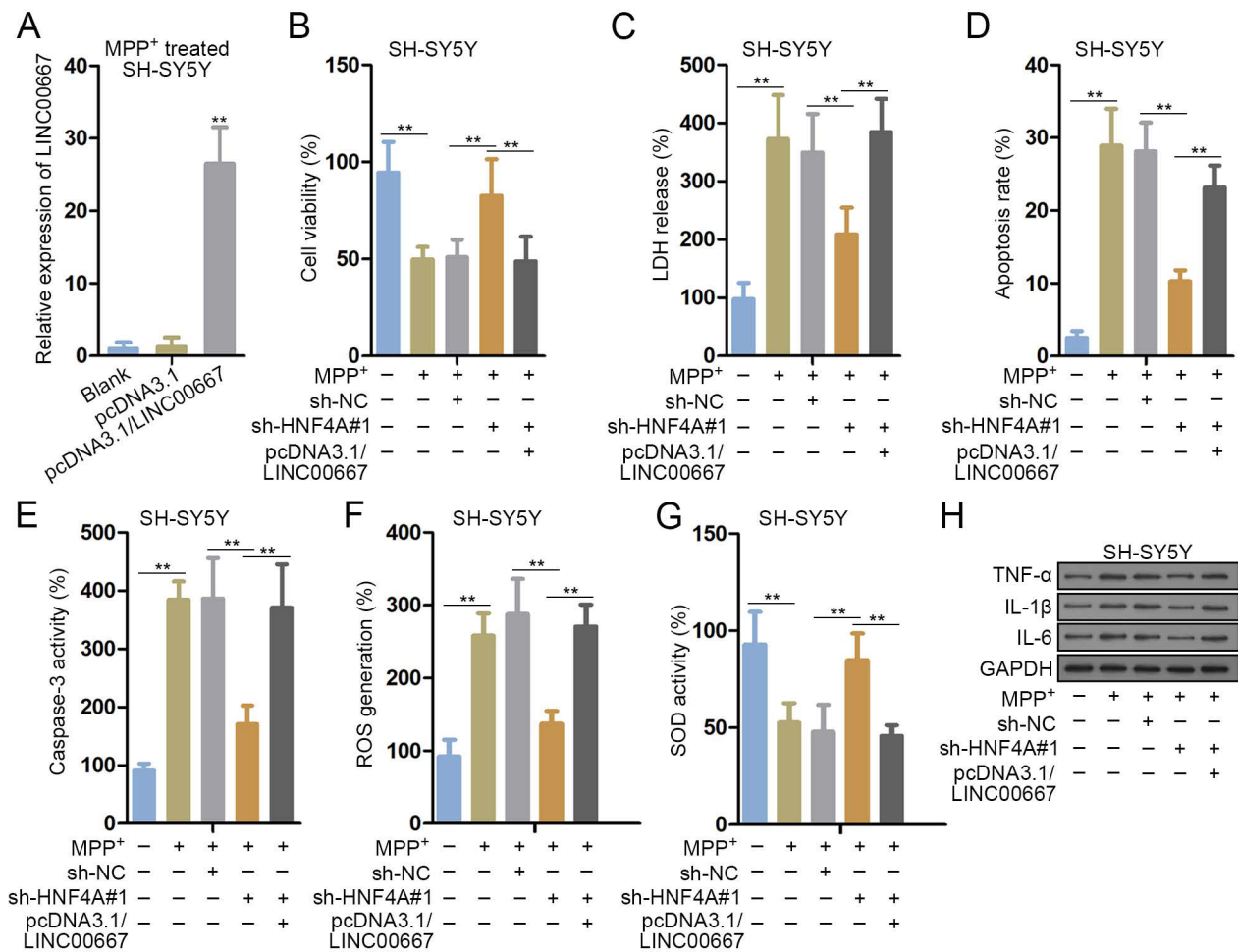


Figure 6. HNF4A-mediated LINC00667 elevation exacerbated MPP⁺-caused neuronal injury. (A) The transfection efficacy of pcDNA3.1/LINC00667 in MPP⁺-treated SH-SY5Y cells was analyzed by qRT-PCR. (B) MPP⁺-intoxicated SH-SY5Y cells were transfected with sh-NC, sh-HNF4A#1, or sh-HNF4A#1+pcDNA3.1/LINC00667; CCK-8 assay was carried out to monitor SH-SY5Y cell viability following multiple treatments. (C) LDH release in specifically treated SH-SY5Y cells was tested. (D and E) Apoptosis rate and caspase-3 activity analyses were examined for SH-SY5Y apoptosis through TUNEL and western blot assays. (F and G) With different conditions, ROS generation, and SOD activity in MPP⁺-treated SH-SY5Y cells were detected. (H) Western blot was carried out to analyze the protein levels of TNF- α , IL-1 β , and IL-6 levels. ***p* < 0.01. HNF4A, hepatocyte nuclear factor 4 alpha; MPP⁺, 1-methyl-4-phenylpyridinium; qRT-PCR, quantitative real-time polymerase chain reaction; LDH, lactate dehydrogenase; TUNEL, terminal deoxynucleotidyl transferase dUTP nick-end labeling; ROS, reactive oxygen species; SOD, superoxide dismutase.

attenuated by LINC00667 elevation (Fig. 6C). Similarly, sh-HNF4A#1-suppressed apoptosis of MPP⁺-intoxicated SH-SY5Y cells was restored by LINC00667 elevation (Fig. 6D and E). Consistently, sh-HNF4A#1-caused decline of ROS generation and promotion of SOD activity could be reversed by the overexpression of LINC00667 (Fig. 6F and G). In western blot, the reduction of TNF- α , IL-1 β , and IL-6 protein resulted from HNF4A deficiency could be recovered by overexpression of LINC00667 (Fig. 6H and Fig. S1F). Altogether, LINC00667 elevation offset the effects of sh-HNF4A#1 on neuronal injury in MPP⁺-intoxicated SH-SY5Y cells.

Discussion

Numerous studies have displayed multiple regulatory genes with aberrant expression in PD. For example, α -synuclein aggregation is pivotal to the pathological processes of PD and it is capable of inducing apoptosis and cytotoxicity in SH-SY5Y cells, thus modulating neuronal injury.²⁶ IGF-1 is involved in miR-126-mediated PD progression.²⁷ Downregulation of DJ-1 induced by microRNA-494 makes cells susceptible to oxidative stress.²⁸ Therefore, to ameliorate neuronal injury is a potential option to understand and treat PD.

Intriguingly, HNF4A has been identified to be increased in PD.^{21,22} Currently, no available information has depicted its function comprehensively. Herein, we established an *in vitro* PD model in SH-SY5Y cells to further confirm the overexpression of HNF4A at a cellular level in PD. Functionally, HNF4A depletion accelerated cell model viability and hindered cytotoxicity as well as cell apoptosis. Meanwhile, loss of HNF4A abrogated MPP⁺-initiated oxidative stress and neuroinflammation. It was uncovered for the first time that HNF4A exerted an effect on PD.

Moreover, miRNAs are a subclass of non-translating or non-encoding RNAs and have gained wide attention in diverse fatal disease studies through posttranscriptional gene repression.²⁹ They have been recognized as potent contributors in PD pathogenesis.^{30,31} According to published research work, downregulated miR-34c-5p is in correlation with great risk of recurrence in laryngeal squamous cell carcinoma.³² MiR-34c-5p facilitates acute myeloid leukemia stem cell eradication through targeting RAB27B to suppress exosome shedding.³³ Aside from that, miR-34c-5p accelerates colon cancer cellular proliferation and curbs apoptosis through targeting SIRT6 to induce the activation of JAK2/STAT3 signaling pathway.³⁴ Present study uncovered that miR-34c-5p directly targeted 3'UTR region of HNF4A mRNA and silenced HNF4A expression. We also found that miR-34c-5p was low expressed in PD cellular model and its elevation led to an increase of cell viability and deduction in cytotoxicity and cell apoptosis. Additionally, miR-34c-5p overexpression abolished MPP⁺-initiated oxidative stress and neuroinflammation. Collectively, our work first demonstrated the involvement of miR-34c-5p in PD and its potent protective role in PD.

lncRNAs are capable of antagonizing the suppression of miRNAs on mRNAs through a ceRNA role.⁷ For example, depletion of lncRNA SNHG1 acts as a ceRNA of miR-137 to alleviate A β ₂₅₋₃₅-induced neuronal injury through modulating KREMEN1 expression in neuronal cells.³⁵ SNHG1 competitively interacts with miR-221/222 cluster and indirectly upregulates p27/mTOR activity in PD.³⁶ LINC00667 has been documented to correlate with small hepatocellular carcinoma overall and recurrence-free survival.¹⁶ Silencing of LINC00667 results in the decline of renal tubular epithelial cell apoptosis and increase of cell proliferation and migration.¹⁴ Herein, we observed that LINC00667 expression was elevated upon MPP⁺ administration in SH-SY5Y cells. Furthermore, it indirectly promoted HNF4A expression through sequestering miR-34c-5p. LINC00667 was discovered to exert a promoting effect in neuronal injury in MPP⁺-intoxicated SH-SY5Y cells. On the other hand, we decided to unravel the mechanism of LINC00667 upregulation and noticed that

HNF4A could serve as a transcriptional driver for multiple genes.^{17–19} Based on bioinformatics information and experimental results, we corroborated that HNF4A transcriptionally upregulated LINC00667 expression via binding to its promoter.

In summary, our work elucidated that LINC00667/miR-34c-5p/HNF4A established a positive feedback loop to aggravate neuronal injury in MPP⁺-intoxicated SH-SY5Y cells, which conferred new therapeutic thoughts in pathological reaction of PD.

Author Contributions

Xinlong Huo was in charge of article organizing. Xinlong Huo, Lisong Wang, and Jiahui Shao were responsible for the experiment. Chenhang Zhou and Xiaowei Ying prepared all the figures. Jinhua Zhao and Xinchun Jin drafted the manuscript. All authors read and approved the final manuscript.

Acknowledgments

All authors thank the experimental help from other participators.

Conflict of Interest

There is no conflict of interest.

References

1. Simon DK, Tanner CM, Brundin P. Parkinson disease epidemiology, pathology, genetics, and pathophysiology. *Clin Geriatr Med.* 2020;36(1):1–12.
2. Xu T-P, Wang W-Y, Ma P, et al. Upregulation of the long noncoding RNA FOXD2-AS1 promotes carcinogenesis by epigenetically silencing EphB3 through EZH2 and LSD1, and predicts poor prognosis in gastric cancer. *Oncogene.* 2018;37:5020–5036.
3. Kalia LV, Lang AE. Parkinson's disease. *Lancet.* 2015;386(9996):896–912.
4. Goetz CG. The history of Parkinson's disease: early clinical descriptions and neurological therapies. *Cold Spring Harb Perspect Med.* 2011;1(1):a008862.
5. Przedborski S, Vila M. The 1-methyl-4-phenyl-1,2,3,6-tetrahydropyridine mouse model: a tool to explore the pathogenesis of Parkinson's disease. *Ann N Y Acad Sci.* 2003;991:189–198.
6. Bergmann JH, Spector DL. Long non-coding RNAs: modulators of nuclear structure and function. *Curr Opin Cell Biol.* 2014;26:10–18.
7. Tay Y, Rinn J, Pandolfi PP. The multilayered complexity of ceRNA crosstalk and competition. *Nature.* 2014;505(7483):344–352.

8. Wang C-J, Zhu C-C, Xu J, et al. The lncRNA UCA1 promotes proliferation, migration, immune escape and inhibits apoptosis in gastric cancer by sponging anti-tumor miRNAs. *Mol Cancer*. 2019;18(1):115.
9. Yang L, Peng X, Li Y, et al. Long non-coding RNA HOTAIR promotes exosome secretion by regulating RAB35 and SNAP23 in hepatocellular carcinoma. *Mol Cancer*. 2019;18(1):78.
10. Mortezaei Z, Lanjanian H, Masoudi-Nejad A. Candidate novel long noncoding RNAs, MicroRNAs and putative drugs for Parkinson's disease using a robust and efficient genome-wide association study. *Genomics*. 2017;109(3–4):158–164.
11. Sengupta S. Noncoding RNAs in protein clearance pathways: implications in neurodegenerative diseases. *J Genet*. 2017;96(1):203–210.
12. Liu Y, Lu Z. Long non-coding RNA NEAT1 mediates the toxic of Parkinson's disease induced by MPTP/MPP+ via regulation of gene expression. *Clin Exp Pharmacol Physiol*. 2018;45(8):841–848.
13. Ni Y, Huang H, Chen Y, Cao M, Zhou H, Zhang Y. Investigation of long non-coding RNA expression profiles in the substantia nigra of Parkinson's disease. *Cell Mol Neurobiol*. 2017;37(2):329–338.
14. Chen W, Zhou Z-Q, Ren Y-Q, et al. Effects of long non-coding RNA LINC00667 on renal tubular epithelial cell proliferation, apoptosis and renal fibrosis via the miR-19b-3p/LINC00667/CTGF signaling pathway in chronic renal failure. *Cell Signal*. 2019;54:102–114.
15. Wang DI, Zheng J, Liu X, et al. Knockdown of USF1 inhibits the vasculogenic mimicry of glioma cells via stimulating SNHG16/miR-212-3p and linc00667/miR-429 axis. *Mol Ther Nucleic Acids*. 2019;14:465–482.
16. Gu J, Zhang X, Miao R, et al. A three-long non-coding RNA-expression-based risk score system can better predict both overall and recurrence-free survival in patients with small hepatocellular carcinoma. *Aging*. 2018;10(7):1627–1639.
17. Liu D, Tang H, Li X-Y, et al. Targeting the HDAC2/HNF4A/miR-101b/AMPK pathway rescues tauopathy and dendritic abnormalities in Alzheimer's disease. *Mol Ther*. 2017;25(3):752–764.
18. Zhou H, Guo L, Yao W, et al. Silencing of tumor-suppressive NR_023387 in renal cell carcinoma via promoter hypermethylation and HNF4A deficiency. *J Cell Physiol*. 2020;235:2113–2128.
19. Zhang X, Xu Y, Qian Z, et al. circRNA_104075 stimulates YAP-dependent tumorigenesis through the regulation of HNF4a and may serve as a diagnostic marker in hepatocellular carcinoma. *Cell Death Dis*. 2018;9(11):1091.
20. Shi J, Dai R, Chen Y, Guo H, Han Y, Zhang Y. LncRNA LINP1 regulates acute myeloid leukemia progression via HNF4alpha/AMPK/WNT5A signaling pathway. *Hematol Oncol*. 2019;37:474–482.
21. Marki S, Goblos A, Szlavicz E, et al. The rs13388259 intergenic polymorphism in the genomic context of the BCYRN1 gene is associated with Parkinson's disease in the Hungarian population. *Parkinsons Dis*. 2018;2018:9351598.
22. Santiago JA, Potashkin JA. Network-based metaanalysis identifies HNF4A and PTBP1 as longitudinally dynamic biomarkers for Parkinson's disease. *Proc Natl Acad Sci USA*. 2015;112(7):2257–2262.
23. Haghi Aminjan H, Abtahi SR, Hazrati E, Chamanara M, Jalili M, Paknejad B. Targeting of oxidative stress and inflammation through ROS/NF-kappaB pathway in phosphine-induced hepatotoxicity mitigation. *Life Sci*. 2019;232:116607.
24. Chen Y, Yang F, Fang E, et al. Circular RNA circAGO2 drives cancer progression through facilitating HuR-repressed functions of AGO2-miRNA complexes. *Cell Death Differ*. 2019;26(7):1346–1364.
25. Klinge CM. Non-coding RNAs: long non-coding RNAs and microRNAs in endocrine-related cancers. *Endocr Relat Cancer*. 2018;25(4):R259–R282.
26. Chen Y, Lian YJ, Ma YQ, Wu CJ, Zheng YK, Xie NC. LncRNA SNHG1 promotes alpha-synuclein aggregation and toxicity by targeting miR-15b-5p to activate SIAH1 in human neuroblastoma SH-SY5Y cells. *Neurotoxicology*. 2018;68:212–221.
27. Kim W, Lee Y, McKenna ND, et al. miR-126 contributes to Parkinson's disease by dysregulating the insulin-like growth factor/phosphoinositide 3-kinase signaling. *Neurobiol Aging*. 2014;35(7):1712–1721.
28. Xiong R, Wang Z, Zhao Z, et al. MicroRNA-494 reduces DJ-1 expression and exacerbates neurodegeneration. *Neurobiol Aging*. 2014;35(3):705–714.
29. Je G, Kim YS. Mitochondrial ROS-mediated post-transcriptional regulation of alpha-synuclein through miR-7 and miR-153. *Neurosci Lett*. 2017;661:132–136.
30. Harratz MM, Dawson TM, Dawson VL. MicroRNAs in Parkinson's disease. *J Chem Neuroanat*. 2011;42(2):127–130.
31. Molasy M, Walczak A, Szaflik J, Szaflik JP, Majsterek I. MicroRNAs in glaucoma and neurodegenerative diseases. *J Hum Genet*. 2017;62(1):105–112.
32. Re M, Magliulo G, Gioacchini FM, et al. Expression levels and clinical significance of miR-21-5p, miR-let-7a, and miR-34c-5p in laryngeal squamous cell carcinoma. *Biomed Res Int*. 2017;2017:3921258.
33. Peng D, Wang H, Li L, et al. miR-34c-5p promotes eradication of acute myeloid leukemia stem cells by inducing senescence through selective RAB27B targeting to inhibit exosome shedding. *Leukemia*. 2018;32(5):1180–1188.
34. Li N, Mao D, Cao Y, Li H, Ren F, Li K. Downregulation of SIRT6 by miR-34c-5p is associated with poor prognosis and promotes colon cancer proliferation through

- inhibiting apoptosis via the JAK2/STAT3 signaling pathway. *Int J Oncol.* 2018;52:1515–1527.
35. Wang H, Lu B, Chen J. Knockdown of lncRNA SNHG1 attenuated Abeta25-35-induced neuronal injury via regulating KREMEN1 by acting as a ceRNA of miR-137 in neuronal cells. *Biochem Biophys Res Commun.* 2019;518(3):438–444.
36. Qian C, Ye Y, Mao H, et al. Downregulated lncRNA-SNHG1 enhances autophagy and prevents cell death through the miR-221/222 /p27/mTOR pathway in Parkinson's disease. *Exp Cell Res.* 2019;384:111614.

Supporting Information

Additional supporting information may be found online in the Supporting Information section at the end of the article.

Figure S1. (A–F) Relative protein levels of targeted proteins detected in Figure 1J, 2O, 3G, 3N, 4H, and 6H were quantified, respectively.

Table S1. Primer sequences used in qRT-PCR analysis among candidate upstream genes of miR-34c-5p were displayed.